

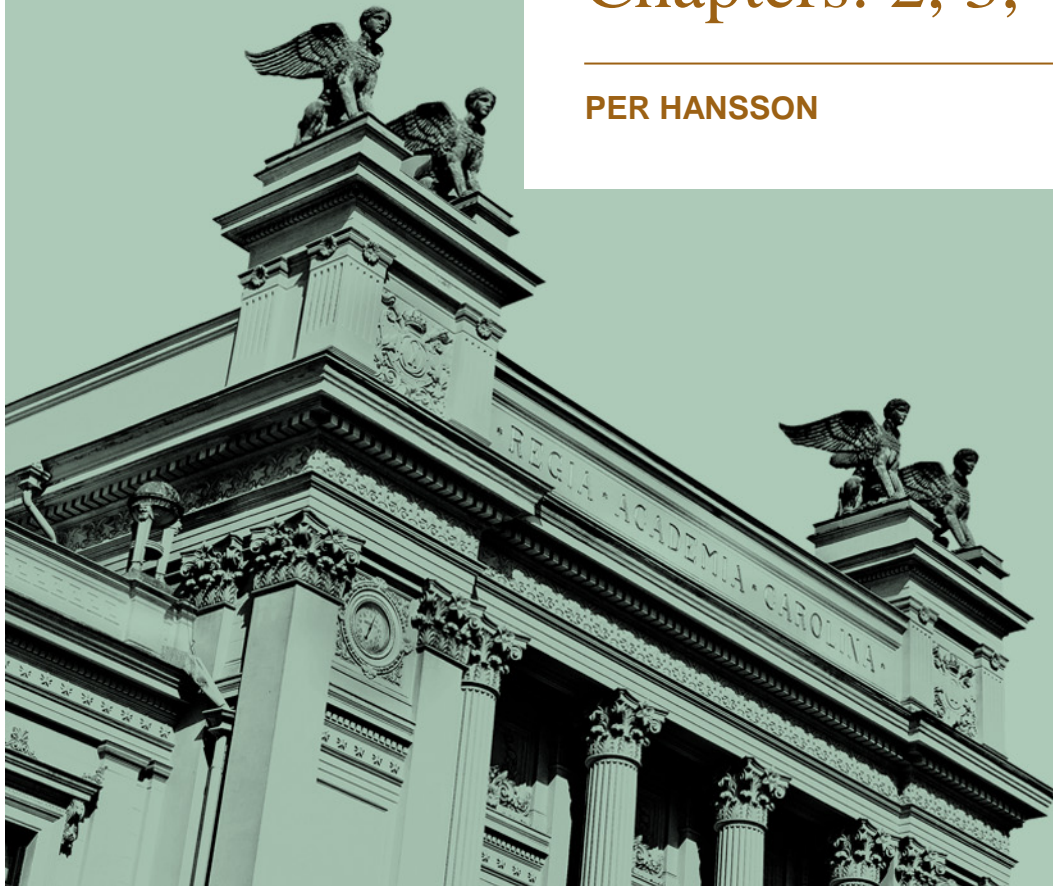


LUND
UNIVERSITY

UTMATTNING, FKM090

Chapters: 2, 3, 4, 10, 14, 15, 16

PER HANSSON



Cyclic deformation and fatigue crack initiation

- Chapter 2. Cyclic deformation in ductile single crystals
 - How does the material behave during cyclic loading?
 - What happens in the material during cyclic loading?
- Chapter 3. Cyclic deformation in polycrystalline ductile solids
 - Differences between single crystals and polycrystals.
- Chapter 4. Fatigue crack initiation in ductile solids
 - Depends on the scale.
 - Different types of initiation.
 - Different causes and starting positions for crack initiation.



1.5 Deformation of ductile single crystals

- Definitions:
 - Resolved shear stress, τ_R
 - Resolved shear strain, γ_R
 - Critical resolved shear stress, τ_c
- The condition for onset of plastic deformation is given by *Schmid law*:

$$\tau_{R_0} = \frac{P}{A} \cos \phi_0 \cos \lambda_0 = \sigma \cos \phi_0 \cos \lambda_0.$$

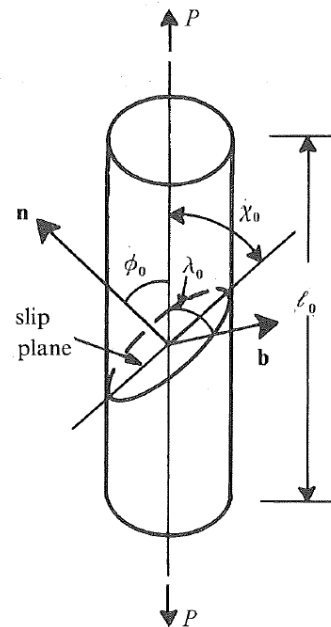


Fig. 1.6. A schematic diagram of a single crystal showing the orientations of the slip plane and the slip direction.

1.5 Deformation of ductile single crystals (2)

- When the cylinder is deformed plastically the geometry changes. Results in an expressions for γ_R and τ_R :

$$\gamma_R = \frac{1}{\cos \phi_0} \left\{ \sqrt{\left(\frac{\ell}{\ell_0}\right)^2 - \sin^2 \lambda_0} - \cos \lambda_0 \right\} \quad \tau_R = \frac{P}{A} \cos \phi_0 \sqrt{1 - (\ell_0 \sin \lambda_0 / \ell)^2}$$

- Rotation of the slip plane and slip direction during deformation

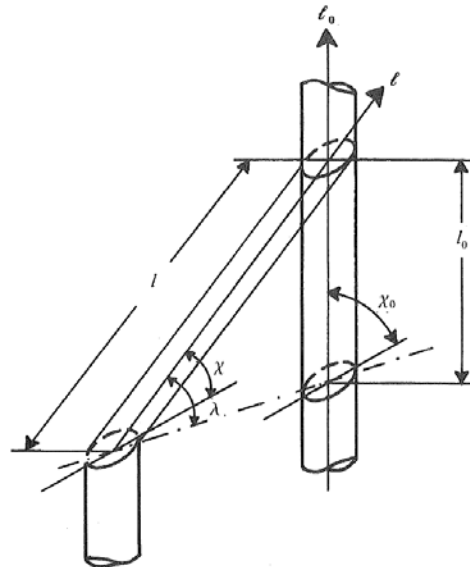


Fig. 1.7. A schematic diagram of change in the gage length vector from ℓ_0 to ℓ due to slip.



1.5 Deformation of ductile single crystals (3)

Stress-strain curve for FCC single crystal, oriented for single slip.

Three stages:

I. After initial elastic deformation. 'Easy glide', primary slip. Slip systems starts to rotate.

II. Secondary slip, increase in work hardening/dislocation density. Cell structures are formed due to cross slip.

III. Increase in cross slip reduces the work hardening effect

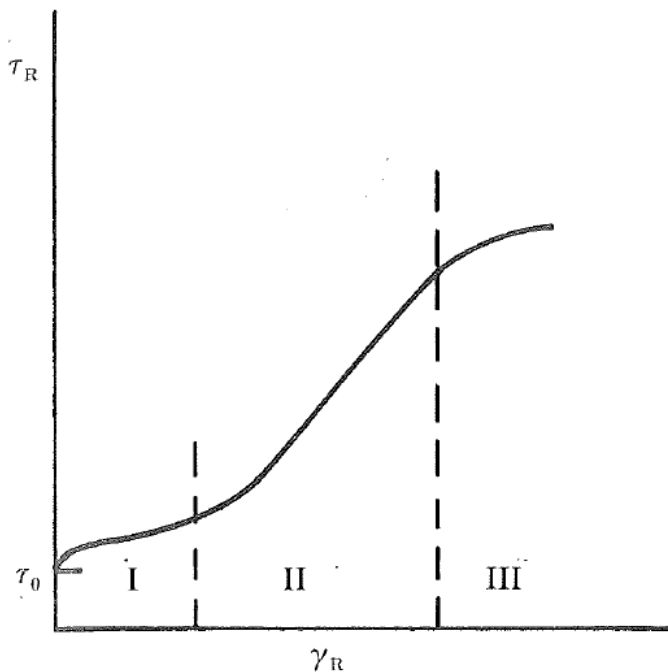


Fig. 1.8. A typical stress-strain curve for an FCC single crystal exhibiting three distinct stages of deformation.



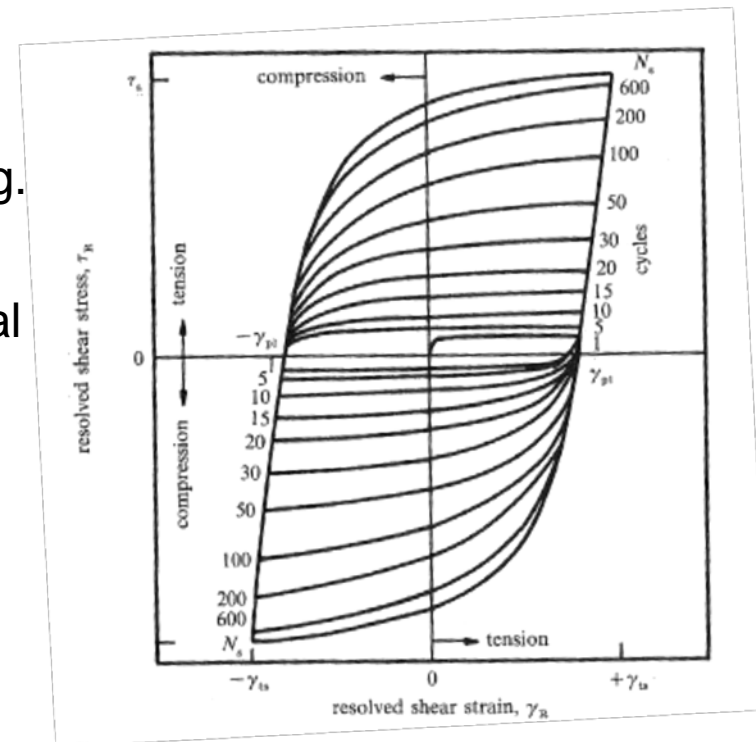
Chapter 2. Cyclic deformation in ductile single crystals

- Been studied since early 1900s
- Found many mechanisms behind the specific behavior under cyclic loading.
- Most conclusive results from studies of single crystals.
- In this course mainly focus on FCC metals



Chapter 2.1. Cyclic strain hardening in single crystals

- Plastic strains are necessary to induce fatigue fracture in ductile single crystals.
- When a FCC single crystal is subjected to cyclic strains rapid hardening is noticed even in the initial cycles.
- After the initial hardening a quasi-steady state occurs, 'saturation'.
- In many cases the plastic shear strain amplitude γ_{pl} is only a fraction of the total strain amplitude γ_t , decreasing with hardening. Most common to perform tests with fixed γ_{pl} .
- A typical hysteresis loop associated with initial hardening and stable loop upon saturation.



Chapter 2.2. Cyclic saturation in single crystals

- Experiments with constant γ_{pl} have shown there exists a saturation stress τ_s, τ_{Rs} .
- Fig. 2.2.a shows stable hysteresis loops (after saturation) for different γ_{pl} .
- Results are used to construct Fig. 2.2b
- Three different regions can be observed:
 - A: Low values of γ_{pl} , work hardening.
 - B: Plateau, τ_s^* independent of γ_{pl} .
 - C: Increase in τ_s^*

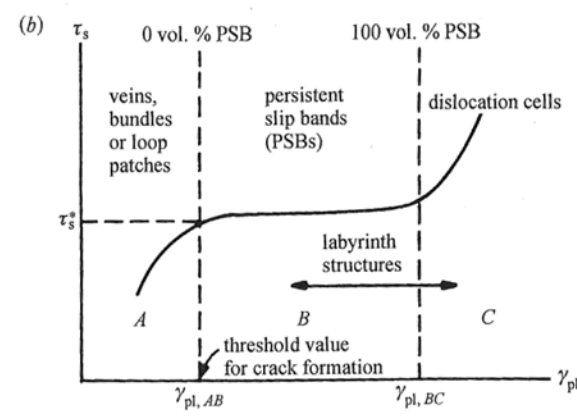
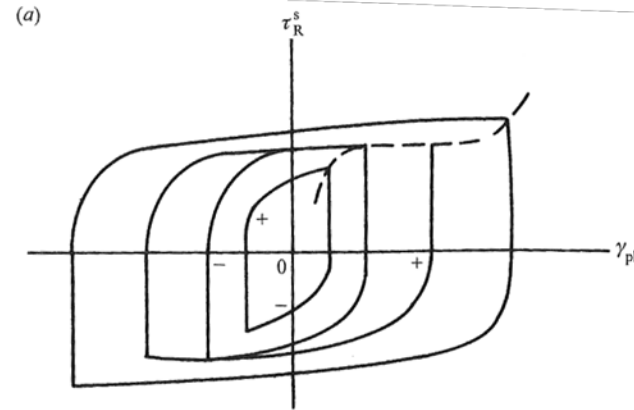


Fig. 2.2. (a) Hysteresis loops with the resolved shear stress at saturation, τ_R^s , plotted against the resolved plastic shear strain, γ_{pl} . The stress-strain curve is drawn through the tips of stable hysteresis loops. (b) A schematic diagram showing different regimes of the saturation stress-strain curve.

Chapter 2.2. Cyclic saturation in single crystals (2)

Table of typical values

Table 2.1. Cyclic stress–strain characteristics of FCC single crystals.

Material	$\gamma_{pl,AB}$	$\gamma_{pl,BC}$	τ_s^* (MPa)	Reference
Cu (523 K)	1.0×10^{-4}	1.0×10^{-3}	14.0	Lisiecki & Weertman (1990)
Cu (295 K)	6.0×10^{-5}	7.5×10^{-3}	27.5	Mughrabi (1978)
Cu (77.4 K)	—	8.0×10^{-3}	48.0	Basinski, Korbel & Basinski (1980)
Cu (4.2 K)	—	—	73.0	Basinski, Korbel & Basinski (1980)
Cu–2.0 Al (at.%) (295 K)	1.0×10^{-4}	3.0×10^{-3}	33.0	Wilhelm & Everwin (1980)
Cu–5.0 Al (at.%) (295 K)	—	—	32.0	Woods (1973)
Cu–16.0 Al (at.%) (295 K)	—	—	20.0–25.0	Li & Laird (1994)
Cu–2.0 Co (at.%) (295 K)	3.0×10^{-4}	5.0×10^{-3}	27.5	Wilhelm & Everwin (1980)
Ni (295 K)	1.0×10^{-4}	7.5×10^{-3}	52.0	Mughrabi, Ackermann, & Herz (1979)
Ni (293 K)	1.0×10^{-4}	8.0×10^{-3}	50.0	Bretschneider, Holste & Tippelt (1997)
Ni (600 K)	7.5×10^{-5}	5.0×10^{-3}	20.5	Bretschneider, Holste & Tippelt (1997)
Ni (750 K)	—	—	12.0–16.0	Bretschneider, Holste & Tippelt (1997)
Ag (295 K)	6.0×10^{-5}	7.5×10^{-3}	17.5	Mughrabi, Ackermann & Herz (1979)
Al–1.6 Cu (at.%) (295 K)	1.5×10^{-5}	1.5×10^{-3}	95.0	Lee & Laird (1983)
Fe–11Ni–16Cr–2Mo (wt%) (295 K)	—	—	59.0	Yan <i>et al.</i> (1986)
Fe–19Ni–11Cr–2Mo (wt%) (295 K)	—	—	59.0	Kaneko, Morita & Hashimoto (1997)



Chapter 2.2. Cyclic saturation in single crystals (3)

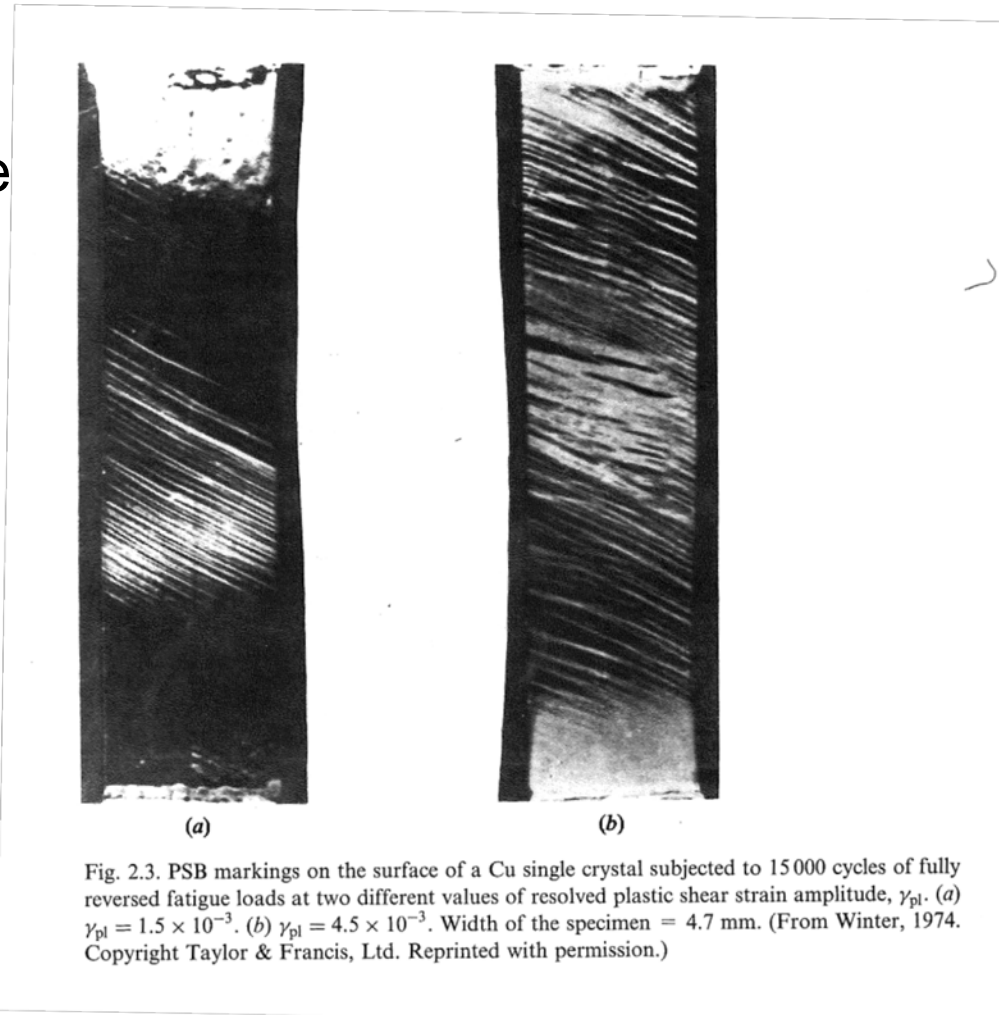
Description of the different regions

- A: Work hardening due to accumulation of primary dislocations. Dynamic equilibrium between bundles of edge dislocations and surrounding screw dislocations. Fine slip markings on the surface. No degenerating damage, can withstand infinite number of fatigue cycles.
- B: Slip along certain bands, persistent slip bands (PSB). Forms through the bulk of the material, reappears at same sites after polishing. PSBs are softer than the surrounding matrix. Fatigue cracks are initiated along PSBs.
- C: Formation of dislocation cells.



Chapter 2.2. Cyclic saturation in single crystals (4)

PSB markings on the surface of a Cu single crystal after 15000 fatigue cycles.



Chapter 2.3. Instabilities in cyclic hardening

- For a single crystal subjected to an increasing stress amplitude (ramp loading) a sequence of minima and maxima in strain amplitude, 'Strain bursts' can be seen.

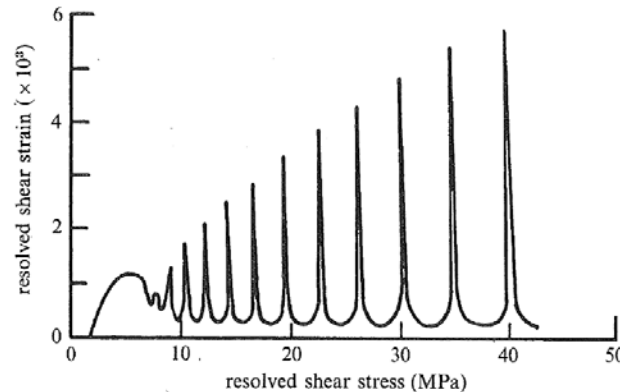


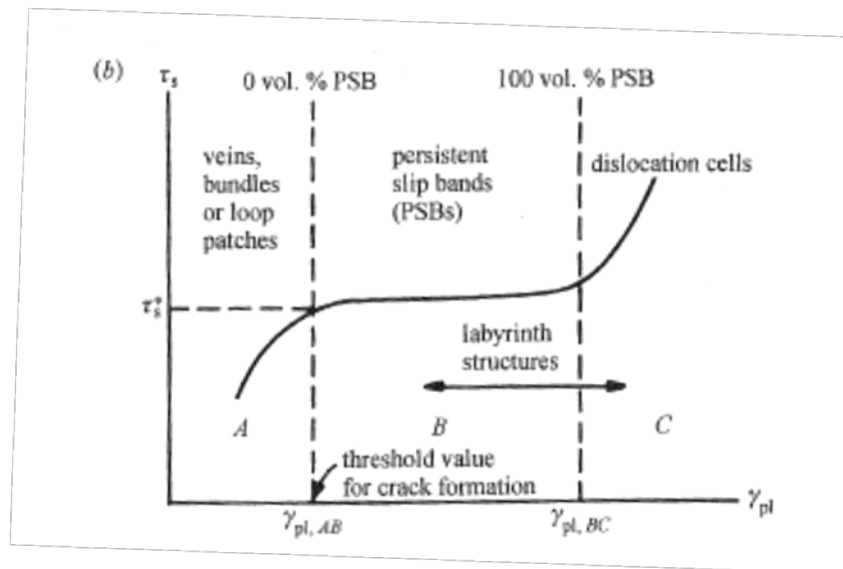
Fig. 2.5. Strain bursts observed in a copper single crystal subjected to increasing stress amplitude at 7.1 kPa/cycle at 90 K. (After Neumann, 1968.)

- Not well defined when they occur, periodic.
- Hardening due to trapping of dislocations reduces γ_{pl} . At sufficiently high stress the dislocation dipoles disintegrate creating an avalanche of free dislocations. Results in large strains 'Strain burst'. At higher stress the dislocations is again trapped.

Chapter 2.3. Instabilities in cyclic hardening (2)

More details about regions A, B and C in Fig. 2.2

- How the vein structure forms, A
- The formation and structure of PSBs, B
- The formation of cell and labyrinth structures, C



Chapter 2.3. Instabilities in cyclic hardening (3)

Formation of dislocation veins

Using TEM the following trends have been found studying cyclic strain hardening in Cu single crystals.

- Dislocations form on the primary glide plane.
- Approximately equal numbers of positive and negative edge dislocations.
- Positive and negative dislocations attract, dipoles are formed until all dislocations have formed dipoles. Only edge dislocations, screw dislocations annihilated by cross slip.
- No internal stresses at long range
- Networks of dipoles are called veins (bundles, loop patches), elongated shape.
- Separated by almost dislocation free channels.



Chapter 2.3. Veinstructure

Vein structure in CU single crystal oriented for single slip, with primary slip vector $[101]$.

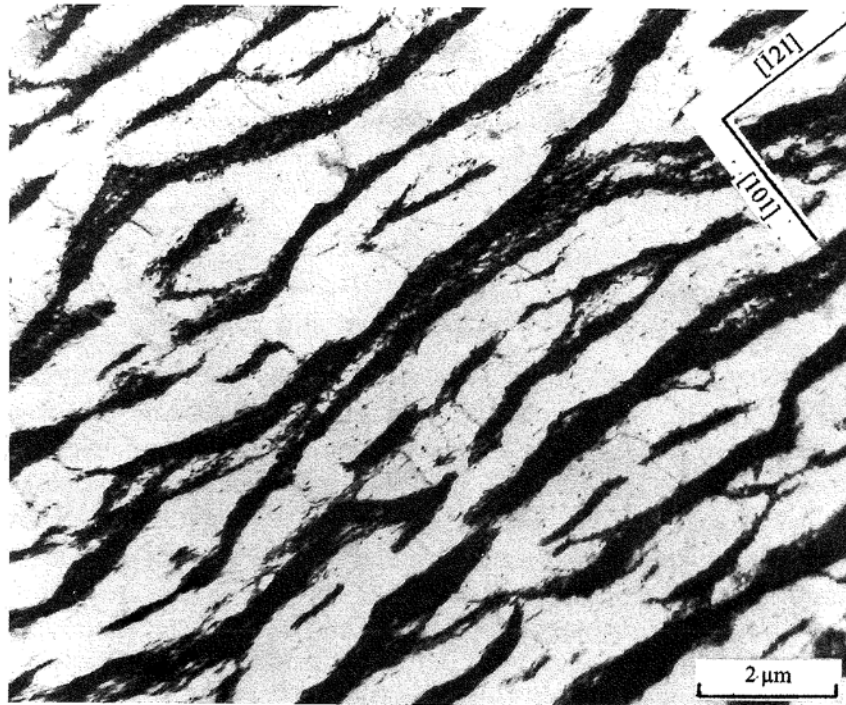


Fig. 2.7. A transmission electron micrograph of matrix vein structure in a section parallel to the primary glide plane of a single crystal of Cu fatigued to saturation at 77.4 K. (From Basinski, Korbel & Basinski, 1980. Copyright Pergamon Press plc. Reprinted with permission.)



Chapter 2.5. Dislocation structure of PSBs

- A PSB is composed of a large number of slip planes (~5000) forming a flat lamellar structure.

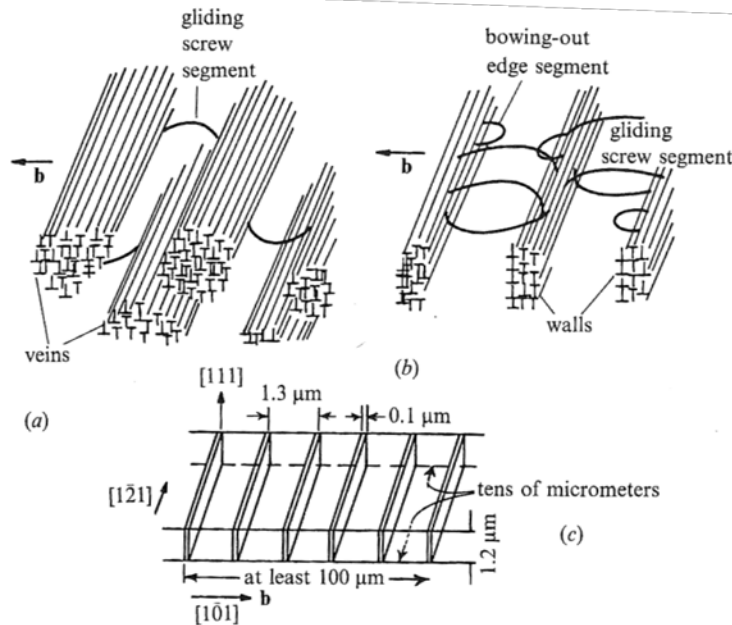


Fig. 2.8. Dislocation arrangements in FCC metals. (a) Vein structure in the matrix. (b) An enlarged view of the dipolar walls and dislocation debris within a PSB. (c) A three-dimension sketch of PSB geometry formed in Cu at 20 °C. (After Mughrabi, 1980, and Murakami, Mura Kobayashi, 1988.)

- A periodic array of dislocation ladders (walls) divides the PSB into channels.
- The walls mainly consists of edge dislocations with its normal in the direction of the primary Burgers vector.
- The dislocation structure in the PSBs and the matrix is considerably different
 - In PSB 10% of the volume is walls of edge dislocations.
 - In the matrix 50% of the volume consists of veins of edge dislocations.

Chapter 2.5. Dislocation structure of PSBs (2)

Three dimensional view of the coexisting PSB and vein structure.

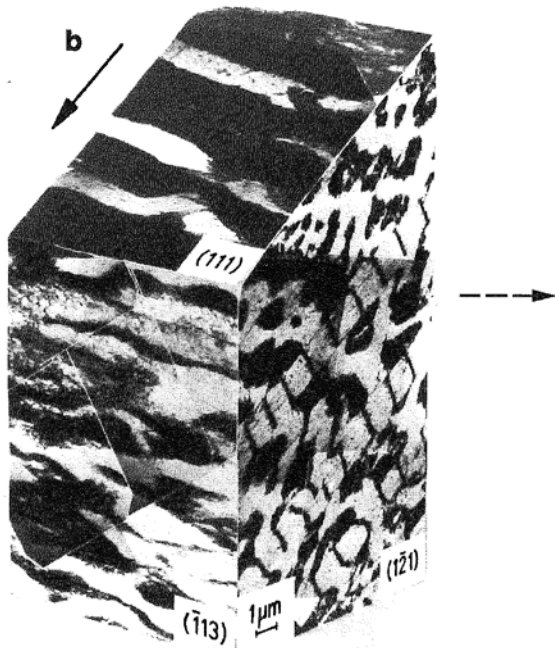


Fig. 2.9. A three-dimensional view, constructed from several TEM images, of the matrix vein and PSB dislocations in Cu cycled to saturation at 20 °C at $\gamma_{pl} = 1.5 \times 10^{-3}$. The specimen loading axis, indicated by the dashed line, is almost on the $(1\bar{2}1)$ plane and it makes an angle of 47° with the primary Burgers vector b . (From Mughrabi, Ackermann & Herz, 1979. Copyright American Society for Testing and Materials. Reprinted with permission.)

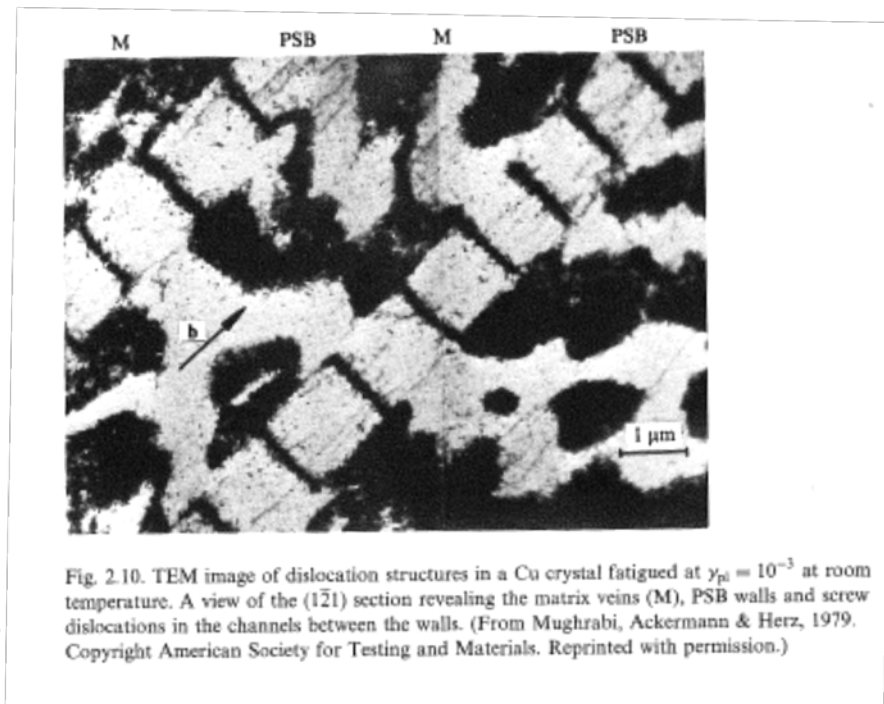
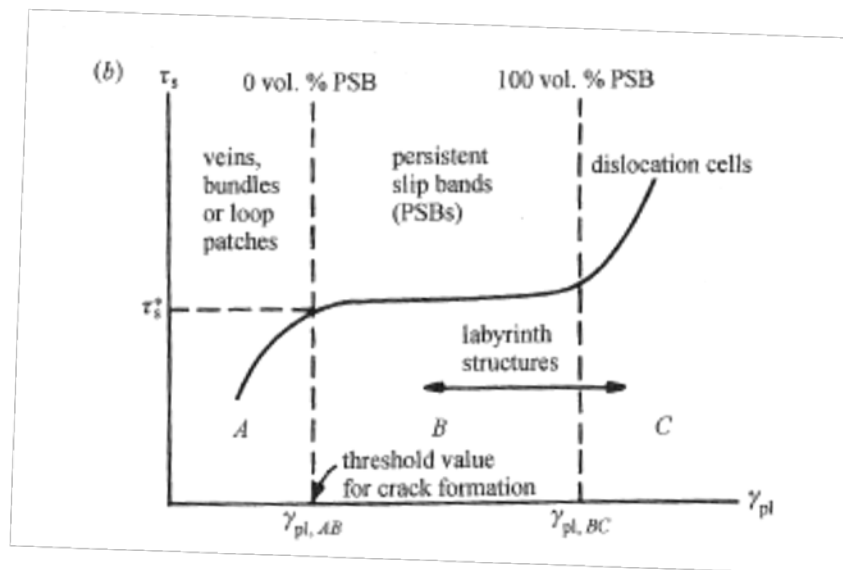


Fig. 2.10. TEM image of dislocation structures in a Cu crystal fatigued at $\gamma_{pl} = 10^{-3}$ at room temperature. A view of the $(1\bar{2}1)$ section revealing the matrix veins (M), PSB walls and screw dislocations in the channels between the walls. (From Mughrabi, Ackermann & Herz, 1979. Copyright American Society for Testing and Materials. Reprinted with permission.)

Chapter 2.5. Dislocation structure of PSBs (3)

Properties:

- PSBs are much softer than the surrounding matrix
- Almost the entire deformation takes place in the PSBs
- Fatigue cracks in single crystals initiate at PSBs. The threshold value τ_s^* is the limit below which fatigue crack initiation does not occur.



Chapter 2.5, 2.7 Formation of PSBs

- In the beginning of part B (Fig 2.2b), structural changes within the matrix must take place to accommodate the high values of γ_{pl} . Have been studied with electron microscope.
- The transformation from veins to PSBs starts in the center of the veins, at small dislocation-poor areas. The soft areas are surrounded by a harder shell with higher dislocation density, creating dislocation walls.
- Each vein transforms to two walls.
- Advanced models describing the phenomena can be found in the book in chapter 2.7.2 and 2.7.3.



Chapter 2.7. Formation of PSBs (2)

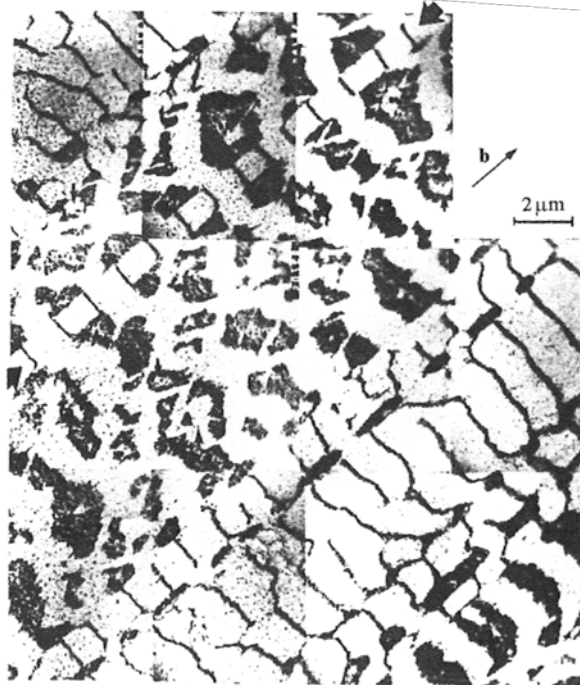
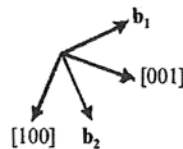
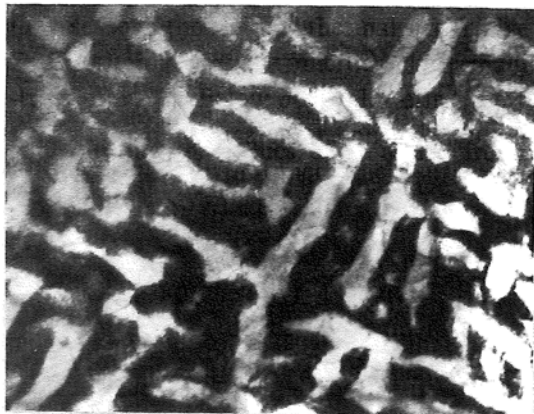


Fig. 2.14. The evolution of a PSB wall structure in the dislocation-poor region of the matrix veins (marked by arrows). $g = (111)$. $\gamma_{pl} = 4 \times 10^{-4}$. (From Holzwarth & Essmann, 1993. Copyright Springer-Verlag. Reprinted with permission.)



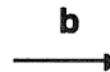
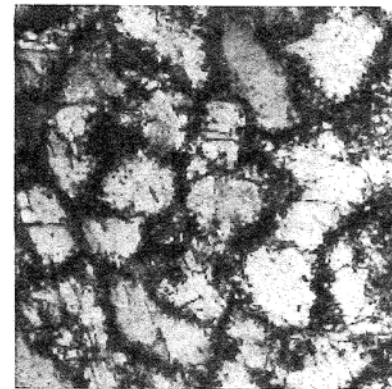
Chapter 2.8. Formation of labyrinth and cell structures

- At higher γ_{pl} an increase in secondary slip occurs. Results in an gradual evolution from PSNs to labyrinth or cell structures.
- Secondary slip starts in the PSB/matrix interface and expands to the entire structure. This is called secondary hardening, region C (Fig. 2.2b).



2 μm

Fig. 2.17. A view of the (010) section of a Cu crystal that was cycled to saturation at $\gamma_{pl} = 5 \times 10^{-3}$, revealing the labyrinth structure. (From Ackermann *et al.*, 1984. Copyright Pergamon Press plc. Reprinted with permission.)



1 μm

Fig. 2.18. A view of the $(1\bar{2}1)$ section of a Cu crystal that was cycled to saturation at $\gamma_{pl} = 1.45 \times 10^{-2}$, revealing cell structures formed by multiple slip in regime C. The primary Burgers vector is along b . (Photo courtesy of H. Mughrabi. Reprinted with permission.)

Chapter 2.11. Monotonic versus cyclic deformation in FCC crystals

- In the first part of the deformation, at low γ_{pl} , the generated dislocation configurations are similar. The difference between the different loading cases increases with increasing γ_{pl} since no PSBs are formed during monotonic loading.
- Differences:
 - Higher dislocation density under cyclic loading
 - No rotation of the slip plane and slip direction during cyclic loading
 - No PSB during monotonic loading, no plateau in the τ_s - γ_{pl} curve.
 - Larger influence of strain rate and temperature under cyclic loading
 - Difference in surface roughness: monotonic-steps
 cyclic- intrusions, extrusions



Chapter 2.11. Monotonic versus cyclic deformation in FCC crystals (2)

Monotonic loading

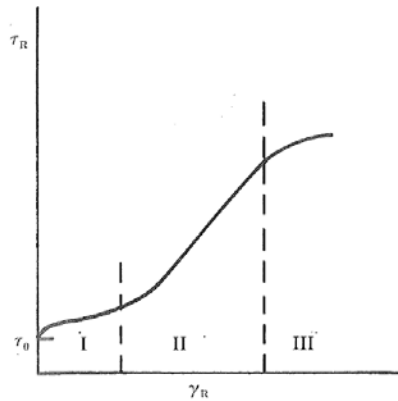
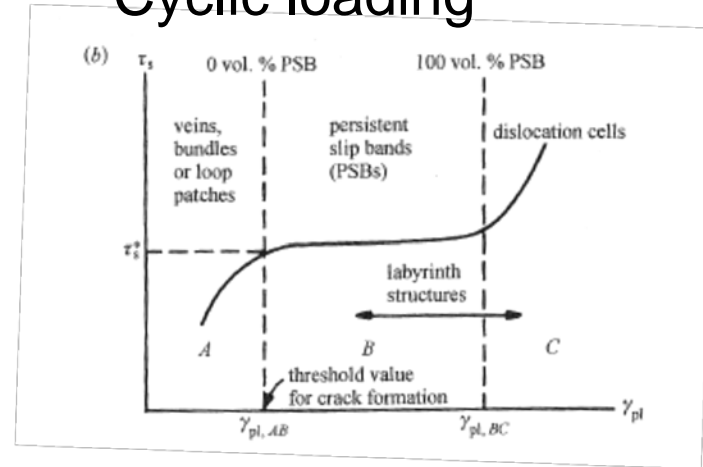


Fig. 1.8. A typical stress-strain curve for an FCC single crystal exhibiting three distinct stages of deformation.

Cyclic loading



Surface roughening

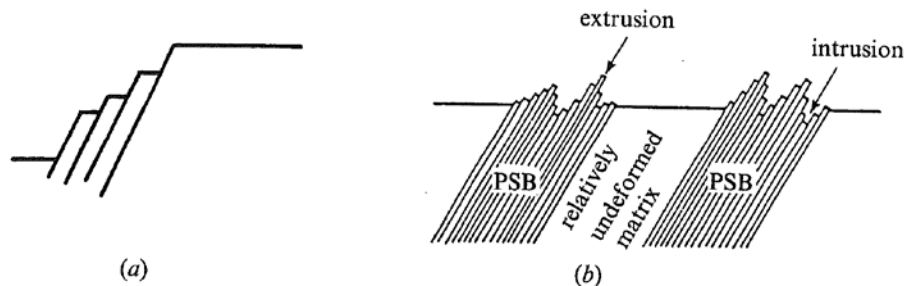


Fig. 2.24. (a) A series of steps resembling a staircase pattern produced by monotonic plastic strain. (b) A rough surface consisting of hills and valleys produced by cyclic plastic strain.



Chapter 2.12. Cyclic deformation in BCC single crystals

- Behaves significantly different from FCC crystals
- The structure of the screw dislocation in BCC crystals induces very high lattice friction (Peierls-stress). Results in:
 - strain-rate sensitivity
 - strong temperature dependence
 - relative mobility of edge and screw dislocation
 - asymmetry between tension and compression
- At low plastic strain amplitudes almost no hardening exists.
- For higher plastic strain amplitudes edge and screw dislocations form a cell structure. The asymmetry results in change of shape of the crystal. No PSBs are formed.
- HCP-Less information is available. More complicated process.

